applied sciences

MDPI

Article

Measurement System for the Experimental Study and Testing of Electric Motors at the Faculty of Engineering, University of Debrecen

Gusztáv Áron Sziki *, Attila Szántó, János Kiss, György Juhász and Éva Ádámkó

Faculty of Engineering, University of Debrecen, H-4028 Debrecen, Hungary
* Correspondence: szikig@eng.unideb.hu

Abstract: The Faculty of Engineering of the University of Debrecen has a long-standing tradition of developing electric and pneumatic-driven prototype race cars. These vehicles are regular participants in domestic and international university competitions. For more conscious development, thus, for more successful racing, a vehicle dynamics simulation program was developed by our research group. One of the main parts of the above program is the simulation of the drive system, including the electric motor. The input data for the motor simulation programs are the electromagnetic and dynamic characteristics of the motor. Most of these characteristics are usually not specified in the motor catalogue; thus, they have to be measured. In this paper, a detailed description of a recently developed measurement system (MS), which is capable of measuring all the above-mentioned characteristics, is presented. Additionally, by applying it, test measurements can also be performed on the motors to check the accuracy of the output functions generated by the simulation programs. Several experimental arrangements and procedures for specific experimental tasks are also presented here as examples for the application of the MS.

Keywords: electric motor; electromagnetic and dynamics characteristics; measurement system; dynamic modelling and simulation

Citation: Sziki, G.Á.; Szántó, A.; Kiss, J.; Juhász, G.; Ádámkó, É. Measurement System for the Experimental Study and Testing of Electric Motors at the Faculty of Engineering, University of Debrecen. *Appl. Sci.* **2022**, *12*, 10095. https://doi.org/10.3390/app121910095

Academic Editor: Andreas Sumper

Received: 23 August 2022
Accepted: 4 October 2022
Published: 8 October 2022

1. Introduction

Nowadays, the contribution of hybrid- and electric-powered vehicles to modern road transport is growing rapidly. Therefore, research on electric [1–3] and pneumatic [4,5] motors applied in them play an increasingly important role, not only in the automotive industry and research institutes but also at universities [5,6].

Adapting to these modern trends, the Faculty of Engineering of the University of Debrecen has been dealing with the development and construction of alternative-driven—primarily pneumatic and electric—prototype race cars for more than a decade [6–9]. With these vehicles, student teams from the faculty regularly participate in various international and domestic competitions. To support the development work, thereby contributing to effective racing, a simulation program [10] has been realized in MATLAB/Simulink environment to compute the dynamics functions (covered distance-, velocity-, acceleration-time functions) of a vehicle from its technical data. An essential part of the above program is the simulation of the drive system, including the electric or pneumatic motor. Regarding electric motors, their electromagnetic and dynamic characteristics serve as input in our [10–13] and other [14–18] simulation modules. The characteristics mentioned above can be, among others, the electric resistance, dynamic self and mutual inductance of motor windings, back EMF, brush voltage, braking torque and moment of inertia of the rotor. Unfortunately, most of these characteristics are not specified in the motor catalogue, so they have to be measured. Primarily, missing parameters has

motivated us to develop a complex measurement system (MS) for the experimental study of electric motors. Another motivation was to be able to check the accuracy of the output functions—generated by the simulation programs—experimentally.

Several different types of electric motor test benches are commercially available, but this equipment is usually developed for specific applications and cannot be modified or developed by the users to serve additional special experimental needs.

In the scientific literature, test benches and measurement systems for electric motors are also presented and described, but the descriptions are usually not detailed enough for the readers to realize those systems.

In Reference [19], a complex measurement system for determining the characteristics of electrical machines is presented. This system can measure all the electrical and mechanical characteristics of the tested motor. Additionally, it is equipped with a control unit and a noise and vibration meter. In Reference [20], a novel and economical motor test bench is presented to measure the electrical and mechanical parameters of single and three-phase AC motors. The test bench can perform the following experimental tasks: load test, no load test, locked rotor test, temperature rise test, losses measurement, measurement of DC resistances of windings, measurement of torque-speed and current speed characteristics. However, Reference [20] does not deal with the study of DC motors. Additionally, it does not provide experimental setups and procedures for measuring the back EMF and the (dynamic) self and mutual inductances of motor windings. In [21], a measurement system is described for determining the flux-linkage and torque characteristics (versus current and rotor position) of switched reluctance machines, but experimental setups and procedures for measuring other motor characteristics are not given. Reference [22] focuses on measuring and evaluating the mechanic, electric and control quantities of AC servo motors and their potential usage in the complex dynamic measurement of mechanism. In [23] and [24], test benches are presented for developing electric vehicle powertrains and for the study of propulsion drives of electric vehicles, respectively. Based on the related scientific literature review, it can be concluded that besides Reference [19], all the presented systems are developed for more specific applications than our system. The "power" and "measurement" units of the system in [19] are similar to the corresponding ones in our equipment (see Section 1), but the technical solutions in many cases are different. It must be emphasized that the description of this system is not detailed enough to make a thorough and detailed comparison, thereby seeing the advantages and disadvantages of the two systems.

In the framework of the Thematic Excellence Programme—launched by the Hungarian Ministry of Innovation and Technology in 2019—several research groups were established at the University of Debrecen in the field of the automotive industry. One of these groups is the Research Group of Vehicle Energetics, which our research group joined in 2019. We could access significant financial support for instrumental developments within the above-mentioned Thematic Excellence Programme framework. Thanks to this support, developments started, and the MS is almost complete now; only minor developments are missing. Applying the MS, all the electromagnetic and dynamic characteristics of an electric motor can be measured. Additionally, test measurements can be performed on it to validate the output functions generated by the developed motor simulation program.

In Section 1, a detailed description of the MS is given, while in Section 2, experimental arrangements and procedures for measuring the dynamics and electromagnetic characteristics of an electric motor and test measurements are presented as examples for the application of the MS.

2. Description of the Measurement System

The described measurement system is entirely designed by the authors. Many of its units and elements are individually manufactured. The authors applied many novel technical solutions during the design and construction. Some of these solutions are the design and configuration of the switch cabinet, using the starting resistor of a tram as a high-power load resistor, the design and configuration of the AC power source with variable voltage and frequency, and the application of the NI 9239 voltage input module as the main instrument in the data acquisition system. During the development, the authors utilized their many years of experience gained during experimental work. Figure 1 shows a photo of the MS consisting of three main units.

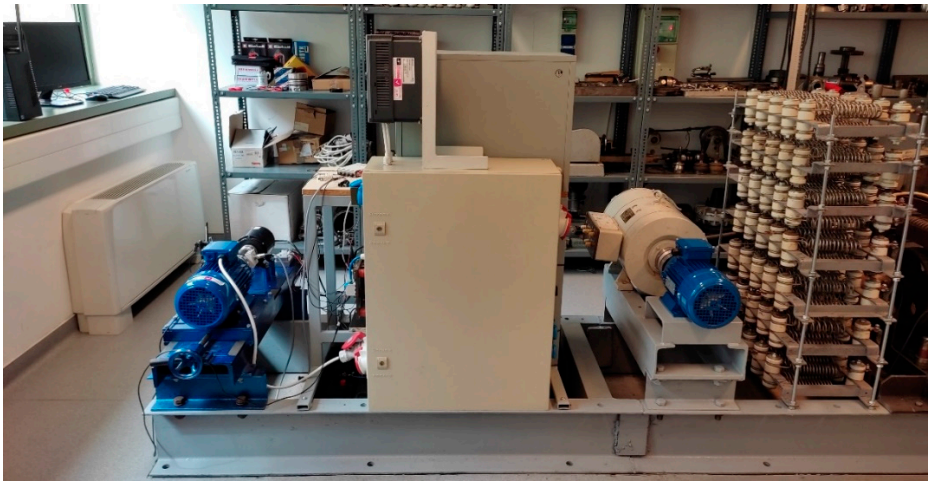

Figure 1. Photo of the measurement system.

These units are:

(1) Motor test bench including the analyzed and load/drive motor together with the connected data acquisition system;
(2) Control desk and switch cabinet, including a special load resistor;
(3) AC power source with variable voltage and frequency.

The following subsections give a detailed description of the units mentioned above.

2.1. Motor Test Bench

Figures 2 and 3 show a schematic diagram and a photo of the motor test bench.

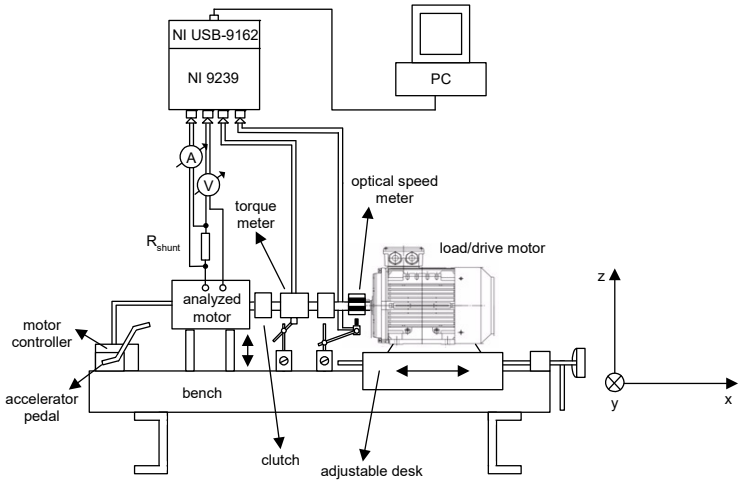

Figure 2. The schematic diagram of the test bench.

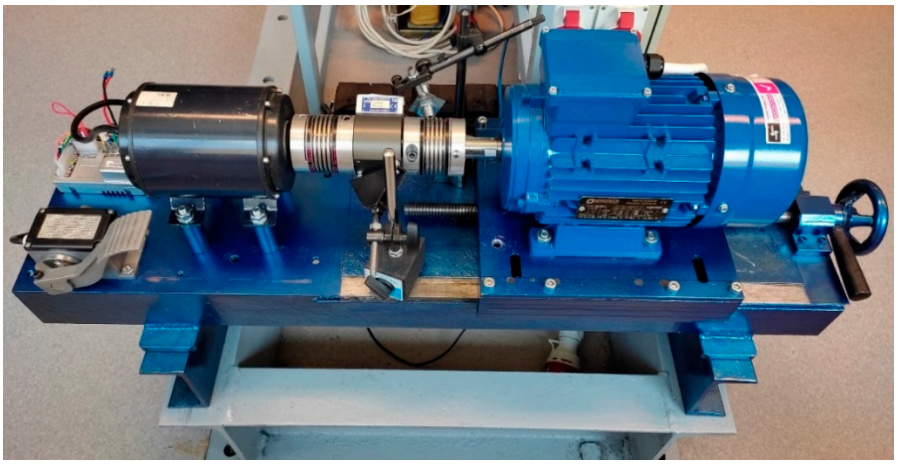

Figure 3. Photo of the test bench.

2.1.1. The Bench, the Analyzed and Load/Drive Motor

The rigid bench is bolted to a welded base frame attached to the floor of the building. The analyzed motor, with its controller and "accelerator pedal", the load/drive motor, the optical LED and rotary torque sensors are fixed to the bench. The analyzed motor can be any kind of electric motor, in certain cases equipped with its controller and "accelerator pedal". It must be emphasized that the controller is not a part of the measurement system; thus, a description of it is not given here. Foot and flanged motors can also be fixed to the bench by applying custom-made adapters. The fixing of the optical LED and rotary torque sensors is solved by magnetic base stand holders. The load/drive motor can be freely moved on the rigid bench in directions x and slightly y, while the analyzed motor is in direction z. Therefore, the proper alignment of the shafts can be adjusted by applying a dial gauge or a laser shaft alignment tool.

The load/drive motor is a three-phase induction motor, and as its name suggests, it has a dual function:

(1) It can be supplied by a variable DC voltage (0–400 V) and used as a "load motor" for braking the analyzed motor.
(2) It can be supplied by a three-phase AC voltage with a variable voltage (0–400V) or frequency (0–50 Hz) and can be used as a "drive motor" for driving the analyzed motor.

2.1.2 Data Acquisition System

In Figure 2, the different parts of the applied data acquisition system are also presented. These parts are:

(1) Optical LED (ROS-P, Monarch Instrument) and rotary torque (HBM T22/200) sensors for angular speed and torque measurement.
(2) Shunt resistor for the measurement of the intensity of the electric current flowing through the windings of the motor.
(3) The voltage input module (NI 9239) and compact DAQ chassis (NI USB 9162) together with a PC.
(4) Self-developed software component for data collection, processing and storing.

The measured torque, angular speed and current intensity are converted to voltage signals by the sensors and the shunt resistor and fed into the NI voltage input module, which is connected to a PC through the Compact DAQ Chassis.

The optical LED sensor operates from a DC power supply (6 V). It provides a $U_{OLS} = 6$ or 0 V output voltage signal depending on whether light is reflected from the rotating object to the sensor. To do this, reflective strips are fixed to the circumference of the rotating object (e.g., to the shaft of the motor). The maximum angular speed which can be measured by the sensor is 25,0000 RPM, but applying more than one strip, this maximum

value is reduced. To check the accuracy of the value measured by the optical led sensor, we measured the speed of the drive motor in the 0–3000 RPM range and compared it with the value shown by the frequency converter. The measured values showed good agreement. The optical LED sensor and its output voltage signals can be seen in Figure 4.

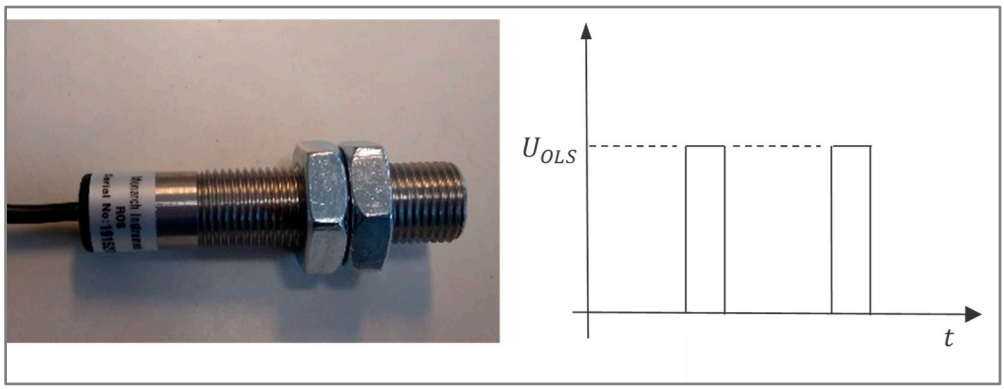

Figure 4. The optical LED sensor and its output voltage signals.

The output voltage signals are counted by applying our self-developed NI LabVIEW program [25], and the angular speed is calculated from the number of strips (N_{strip}) and the number of detected voltage signals (N_{signal}) in a short Δt time using the following formula:

$$\omega = \frac{2\pi}{\Delta t} \cdot \frac{N_{signal}}{N_{strip}} \quad (1)$$

The rotary torque sensor is connected to the analyzed and load/drive motors through clutches. The size of the applied clutches depends on the maximum possible torque delivered by the motors to the sensor. The applied torque sensor has a nominal (rated) torque of 200 Nm, and its accuracy class is 0.5%. (It must be emphasized that the T22 torque meter is available with rated torques varied in the range of 0.5–1000 Nm.) The torque measured by the sensor is linearly proportional to its output voltage, and it is 200 Nm at 5 V (Figure 5).

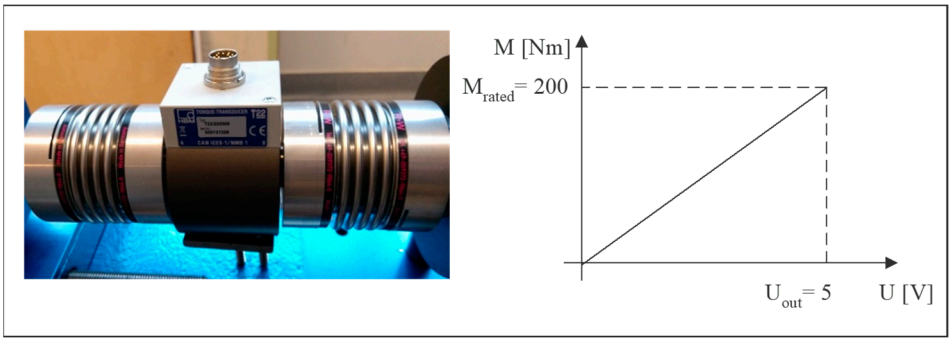

Figure 5. The rotary torque sensor and its output voltage signal.

Two shunt resistors (Figure 6) with voltage drops of 60 and 75 [mV] at 100 and 300 [A] nominal current intensities are used for measuring the intensity of the electric current flowing through the windings of the analyzed motor. Thus, the maximum current intensities we can measure safely are 100 and 300 [A], respectively.

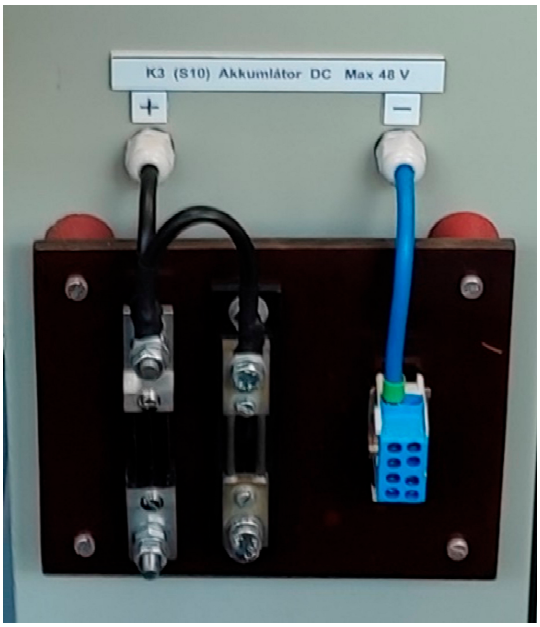

Figure 6. Shunt resistors for measuring the electric current intensity.

The NI 9239 voltage input module has four channels with an allowed input voltage range of −10 V to 10 V for each channel. If the voltage to be measured is outside this range, a voltage divider with a division ratio of 1:11 is used. The module's maximum sample rate and analog input resolution are 50 kHz and 24 bits, respectively. The module has an analog input isolation on a channel-to-channel basis; thus, the entire system is protected from harmful voltage spikes up to the isolation rating. In addition to safety, isolation eliminates measurement errors caused by ground loops because the front end of the module is floating. The voltage input module is connected to the PC through an NI USB-9162 device (National Instruments, Debrecen, Hungary), which is a Single-Module Carrier Compact DAQ Chassis. The self-developed software component of the MS is implemented in NI LabVIEW, Java SE and VBA with an underlying MySQL database. Applying the software component, the measured quantities can be monitored in real time, displayed graphically, and stored in a database for later use. A detailed description of the software component can be found in Reference [25].

2.2. Switch Cabinet, Control Desk and Load Resistor

To operate the electric devices (analyzed motor, load/drive motor, frequency converters, sensors, battery charger) in the MS, appropriate power sources are necessary. A multifunctional switch cabinet and a control desk were developed to ensure them. Figure 7 shows a photo of the above equipment.

Figure 7. The electrical switch cabinet and control desk.

In Figure 8, photos of the inside (**a**) and outside (**b**) of the switch cabinet are presented. The photos have been labelled for a more straightforward description.

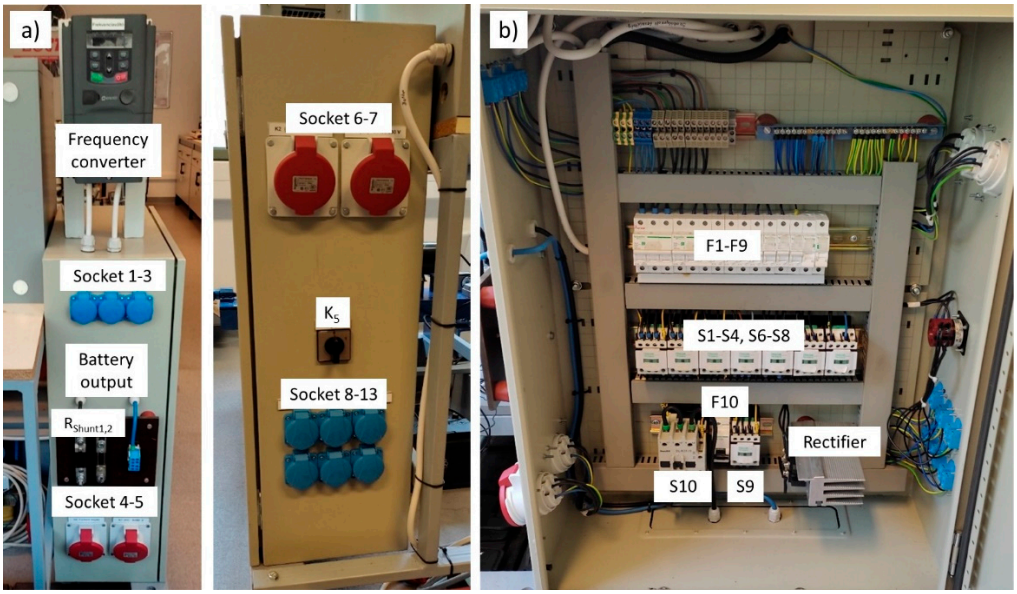

Figure 8. Side-view photos of the switch cabinet from outside (**a**) and its interior design (**b**).

The contactors S1-S4, S6-S9 and S10, the fuses F1-F10, and the rectifier are built in the switch cabinet. Contactor S5 is built into the control desk. The user can operate the switch cabinet from the control desk (Figure 9).

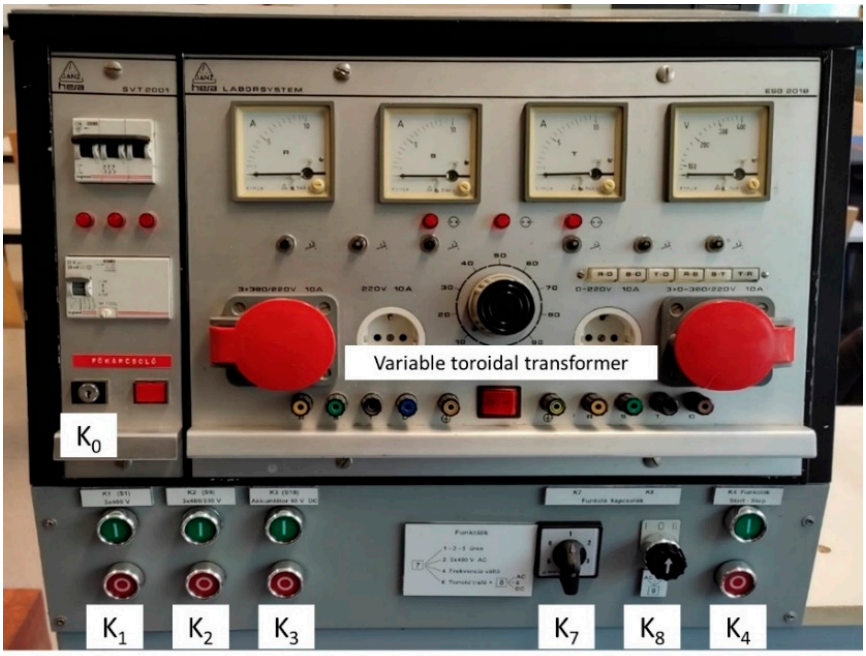

Figure 9. Labelled photo of the control desk (panel).

In Figures 10 and 11, the wiring diagrams of the switch cabinet and the control panel are presented.

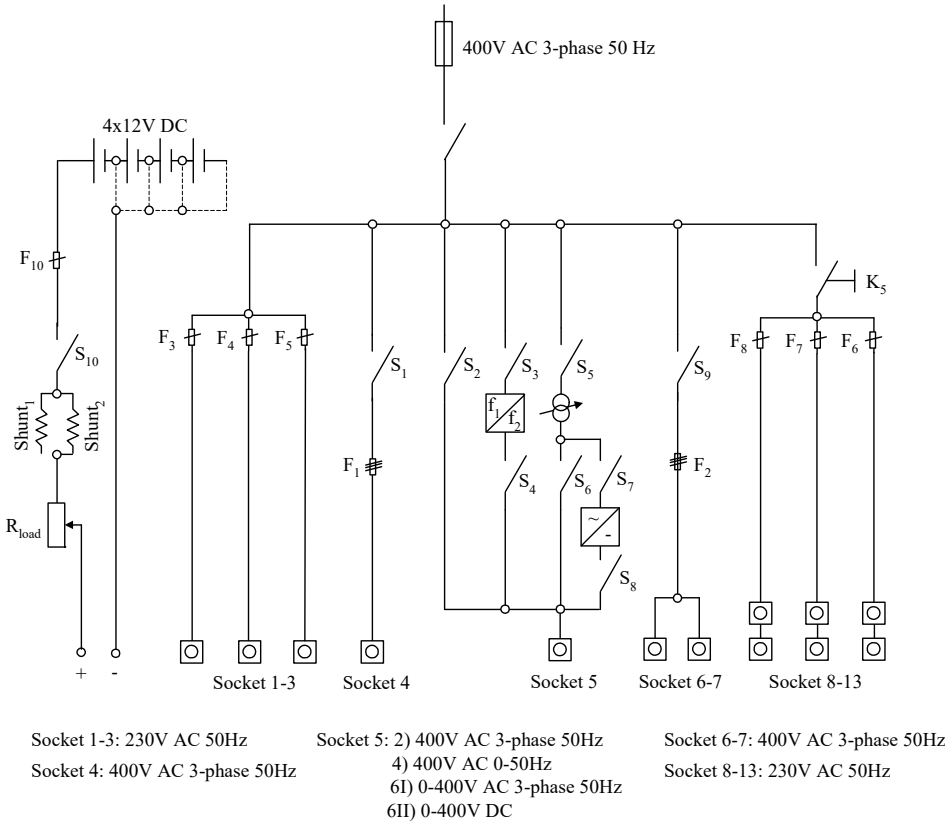

Figure 10. Wiring diagram of the switch cabinet and control panel (diagram 1).

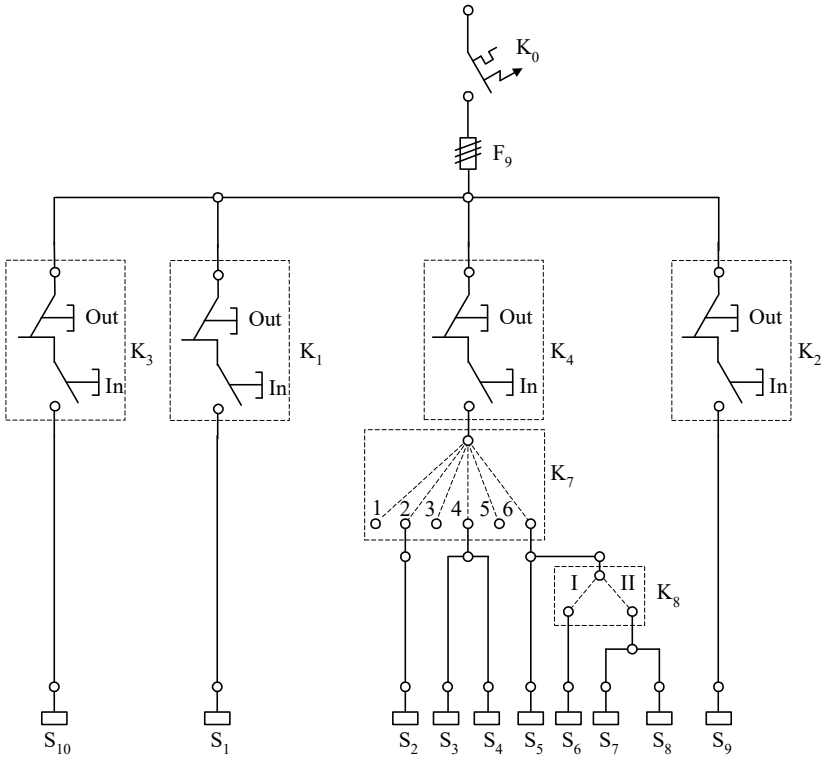

Figure 11. Wiring diagram of the switch cabinet and control panel (diagram 2).

In Figures 10 and 11, S_1,.., S_{10} and F_1,…, F_{10} are contactors and fuses, while K_0,…, K_5, K_7, K_8 are switches and R_{load}, R_{shunt1}, R_{shunt2} are the load and shunt resistors. From the wiring diagrams, the following combinations can be read:

(C1) If switch K_0 is closed, sockets 1–3 are supplied with 230 V 50 Hz AC.
(C2) If switches K_0 and K_5 are closed, sockets 8–13 are supplied with 220 V one-phase 50 Hz AC.
(C3) If switches K_0 and K_1 are closed, socket 4 is supplied with 400 V three-phase 50 Hz AC.
(C4) If switches K_0 and K_2 are closed, sockets 6–7 are supplied with 400 V three-phase 50 Hz AC.
(C5) If switches K_0, K_4 and $K_{7,2}$ are closed, socket 5 is supplied with 400 V three-phase 50 Hz AC.
(C6) If switches K_0, K_4 and $K_{7,4}$ are closed, socket 5 is supplied with 400 V three-phase AC with a variable frequency between 0 and 50 Hz. Changing the frequency is solved by the frequency converter in Figure 8a.
(C7) If switches K_0, K_4 and $K_{7,6,I}$ are closed, socket 5 is supplied with three-phase AC with a variable voltage between 0 and 400 V. Changing the voltage is solved by the variable toroidal transformer in Figure 9.
(C8) If switches K_0, K_4 and $K_{7,6,II}$ are closed, socket 5 is supplied with DC with a variable voltage between 0 and 400 V. Changing the voltage is solved by the variable toroidal transformer in Figure 9. The rectifier can be seen in Figure 8b.
(C9) If switches K_0 and K_3 are closed, we can use DC, which is obtained from four car batteries. Changing the resistance of the load resistor (0–7 Ω) , the intensity of the electric current in the circuit can be varied.

The load resistor is a high-power resistor originally used as a starting resistor of a tram. Thus, it can be applied at very high current intensities.

Combinations C1–C5 can be used for everyday applications, while C6 and C8 can be used when we use the three-phase induction motor (Figures 2 and 3) as a drive and load motor, respectively. Combination C7 can be used to provide supply voltage to an AC, while C6 and C9 to a DC motor. It must be emphasized again that the analyzed motor can be any type of AC or DC motor. Combination C9 can also be used for investigations when a direct current with strictly constant—but wide-range variable—intensity is necessary. One example is the measurement of the mutual dynamic inductance between the stator and rotor windings of a series-wound DC motor [26]. Another example is when an electric current with a strictly constant intensity is necessary for the measurement of the pure electric resistance of a winding.

2.3. AC Power Source with Variable Voltage and Frequency

The schematic diagram of the AC power source is shown in Figure 12.

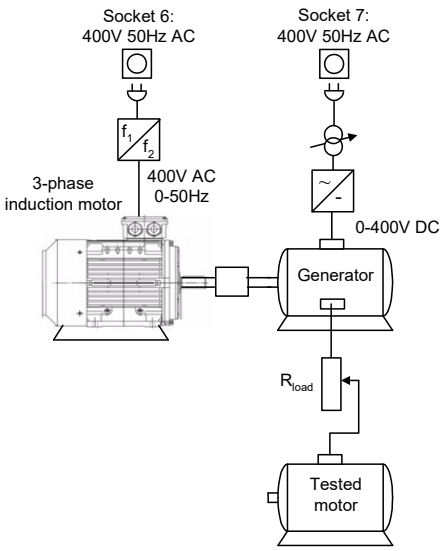

Figure 12. Schematic diagram of the AC power source with variable voltage and frequency.

The power source produces a clean sinusoidal three-phase AC with variable voltage and frequency (typically 5–50 Hz) on its output. To realize this, an externally excited synchronous generator (the stator windings are excited by variable DC) is driven by a three-phase induction motor supplied by a three-phase AC through a frequency converter. The output frequency of the power source (5–50 Hz) is adjusted by the frequency converter, while its output voltage is by the variable DC on the stator windings of the synchronous generator. It has to be emphasized that for experimental work, only one phase is used from the three output phases of the power source. The application of the power source is presented in Section 2, and photos of it are in Figure 13.

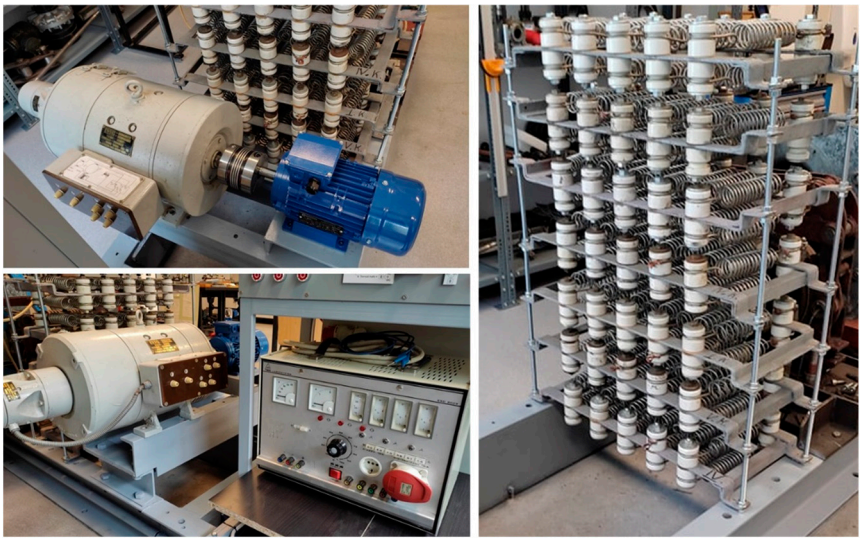

Figure 13. Photos of the AC power source and the load resistor.

3. Applications of the Measurement System

The authors have developed the measurement system for the experimental study of electric motors applied in vehicle drives. So far, a 4 kW series-wound DC motor has been studied, and the investigation of an 800 W brushless DC motor is in progress. The measurement system has numerous applications, some of which are presented here as examples. The measured characteristics so far are the electric resistance, dynamic self- and mutual inductance of motor windings (2), brush voltage, braking torque and moment of inertia of the rotor. The detailed description of the experimental and evaluation procedures, together with the application of the measured characteristics for modelling and simulation purposes, are described in detail in [26] and [27]. It should be emphasized that the range of applications is expanding, and some new applications may require further development of the measurement system. Current applications can be divided into two groups:

(1) The measurement of the dynamics and electromagnetic characteristics of an electric motor.
(2) Test measurements on an electric motor.

As mentioned before, the dynamics and electromagnetic characteristics serve as input data for the motor simulation modules, while the test measurements are applied to check the accuracy of the output functions generated by the simulation modules. In Section 2.1, examples for the first are given, while in Section 2.2, examples are given for the second group. Some of the examples can be applied to any type of electric motor, while others only to particular motor types. In the second case, the type of the motor is specified when the application is described.

3.1. Measurement of Dynamics and Electromagnetic Characteristics

3.1.1. Measurement of Braking Torque and Moment of Inertia

Figure 14 shows an experimental setup for measuring the braking torque on the rotor of an electric motor vs. its angular speed.

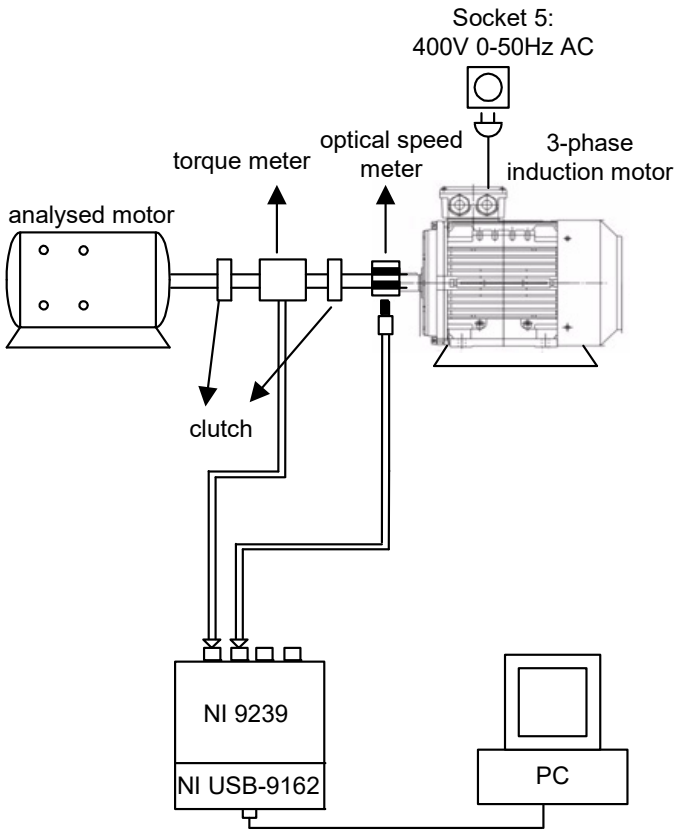

Figure 14. Experimental setup for the measurement of the braking torque on the rotor of an electric motor.

The braking torque includes the bearing, the windage and the brush friction torques and may include other kinds of torques depending on the type of the motor. During the measurement, the three-phase induction motor is connected to Socket 5 and used as a "drive motor" (C6, Section 2.2).

Experimental Procedure

Applying the frequency converter, the speed of the "drive motor" is increased in small, equal steps from zero. At each step, the angular speed and the torque on the rotor of the analyzed motor are measured. (During the measurements, the angular acceleration of the rotor is zero.) After that, the measured torque can be given versus the measured angular speed. Since the measured torque is the braking torque of the rotor, finally, we obtain the function $M_{brake}(\omega)$. It must be emphasized that the measurement of the braking torque, when applying the above procedure, is only possible if a torque meter with a very low nominal (rated) torque and value of accuracy class is applied (typically: <0.5 Nm and <0.5%). If such a torque meter is unavailable, or if we do not have a torque meter, the experimental setup and procedure in References [28,29] for the simultaneous measurement of the braking torque and moment of inertia can be applied.

In Figure 15, an experimental setup for measuring the moment of inertia of the rotor of an electric motor is presented.

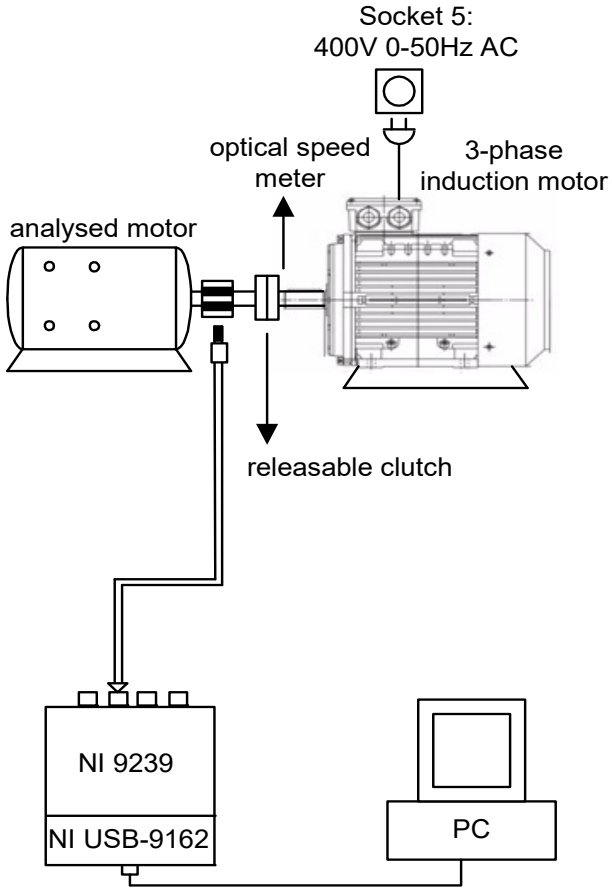

Figure 15. Experimental setup for the measurement of the moment of inertia of the rotor of an electric motor.

Experimental Procedure

During the measurement, the three-phase induction motor is plugged into Socket 5 and used as a "drive motor". Its shaft is connected to the shaft of the analyzed motor through a releasable clutch. Applying the frequency converter, the speed of the "drive motor" is increased until it reaches its maximum speed. After that, the clutch is released, and the rotor of the analyzed motor slows down until it stops. During the retardation, its angular speed is measured by the optical LED sensor. From the measured angular speed vs. time function, its angular acceleration vs. time function can be calculated by derivation. After that, its angular acceleration can be given as the function of its angular speed ($\varepsilon(\omega)$). From function $\varepsilon(\omega)$ and the previously measured $M_{brake}(\omega)$ function, the moment of inertia of the rotor can be calculated as:

$$J_{rotor} = \frac{M_{brake}(\omega)}{\varepsilon(\omega)} \quad (2)$$

In the case of a successful experiment, the calculated moment of inertia has a constant value in a wide angular speed range.

3.1.2. Measurement of the Electric Resistance, Dynamic Self and Mutual Inductance of Motor Windings

Figure 16 shows an experimental setup for measuring the electric resistance of the stator or rotor winding of an electric motor.

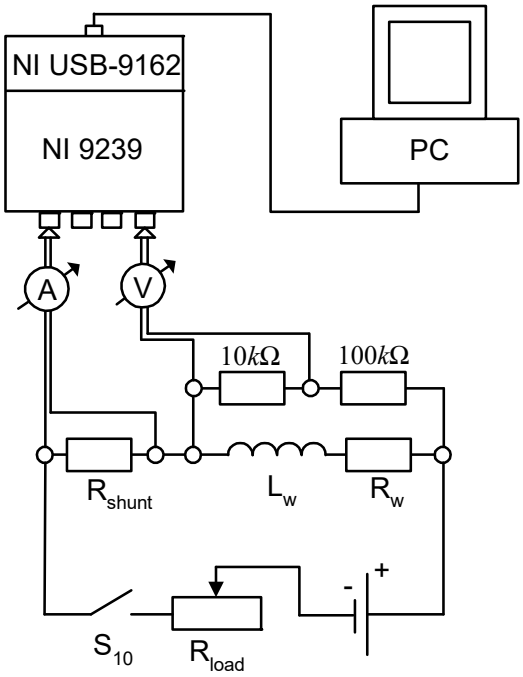

Figure 16. Experimental setup for measuring the electrical resistance of motor windings.

Experimental Procedure

In the figure, R_w and L_w denote the electric resistance and inductance of the winding. During the experiment, the voltage drops on the winding (U_w) and the shunt resistor (U_{shunt}) are measured at constant current intensity. The intensity of the current flowing through the winding (I_w) can be calculated from the voltage drop on the shunt resistor. Varying the intensity of the current with the variable load resistor, U_w can be given as a function of I_w. If the heating of the winding and shunt resistor is negligible, this function is linear, and its slope gives the electric resistance of the winding. It must be emphasized that in the case of a brushed motor, the voltage drop on the rotor winding cannot be measured through the carbon brushes. If we do this, the brush voltage will also be included, and the function mentioned above will not be linear. The details of this phenomenon and the measurement procedure of the brush voltage can be found in References [26,30].

In Figure 17, an experimental setup for measuring the self-dynamic inductance of a motor winding is presented.

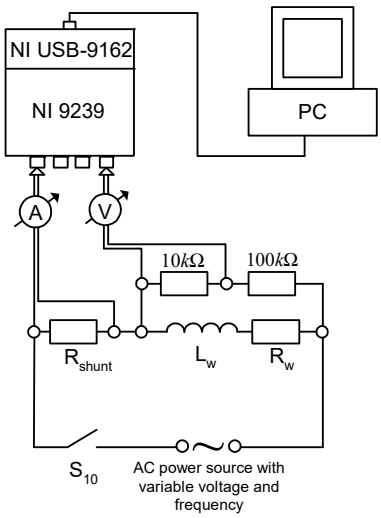

Figure 17. Experimental setup for measuring the self-dynamic inductance of a motor winding.

Experimental Procedure

The winding of the analyzed motor is excited by the AC power source presented in Section 2.3. During the measurement, the voltage drops on the shunt resistor (U_{shunt}) and the winding (U_w) are measured as the function of time. From the voltage drop on the shunt resistor, the current intensity through the winding (I_w) can be calculated. After that, the magnetic flux over the winding is calculated by the following formula:

$$\psi_w(t) = \int_0^t \left(U_w(t) - R \cdot I_w(t)\right) \cdot d\tau + \psi_w(0) \quad (3)$$

From the $\psi_w(t)$ and $I_w(t)$ functions, the self-dynamic inductance can be calculated as a function of current intensity $\left(L_w(I_w)\right)$. The detailed mathematical procedure is presented in [26], together with experimentally determined self-dynamic inductances for a series-wound DC motor. The application of these inductances as input characteristics of a motor simulation program module is also presented in [26].

Figure 18 shows an experimental setup for measuring the mutual dynamic inductance between the stator and rotor windings of a series-wound DC motor.

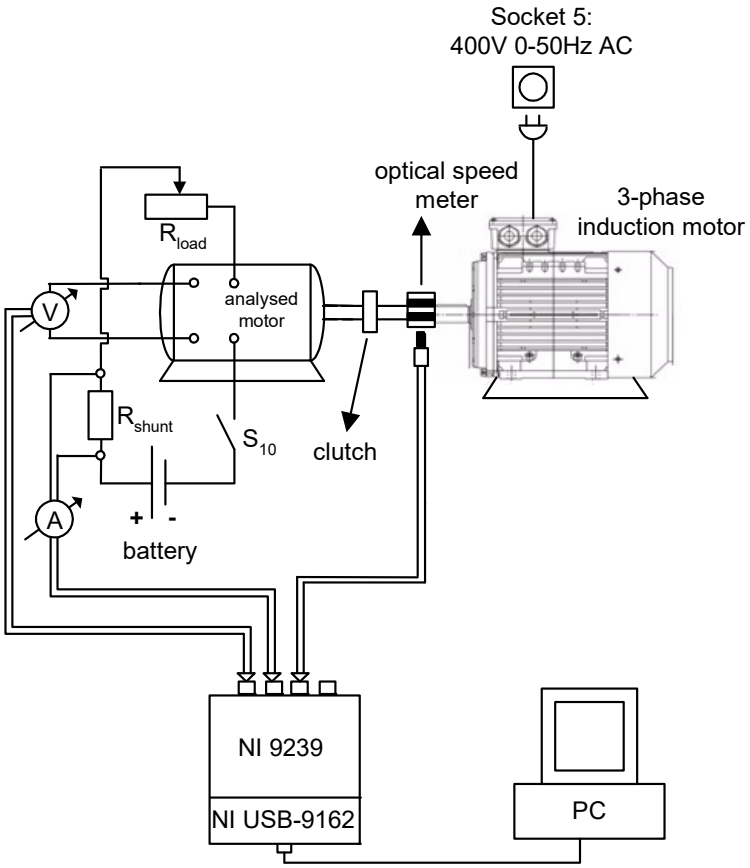

Figure 18. Experimental setup for measuring the mutual dynamic inductance between the stator and rotor windings of a series-wound DC motor.

Experimental Procedure

The stator and rotor windings have to be electrically disconnected during the measurement. The stator winding is supplied with direct current. The armature winding is rotated at a fixed, constant angular speed ω in the magnetic field of the stator winding, and the voltage (U_{rw}) induced in it is measured. For rotating the armature winding, the three-phase induction motor is used in the "drive motor" mode (C6, Section 2.2). The intensity of the current flowing through the stator winding (I_{sw}) is varied, by adjusting

the resistance of the load resistor (R_{load}). The mutual dynamic inductance can be calculated from the quantities above according to the following formula:

$$L_{s,r} = \frac{U_{rw}}{\omega \cdot I_{sw}} \tag{4}$$

It must be emphasized that at a given I_{sw} current intensity, the $\frac{U_{rw}}{\omega}$ ratio is independent of the value of ω. Thus, the mutual dynamic inductance is a motor characteristic which depends only on the intensity of the current flowing through the motor. The experimentally determined mutual dynamic inductance for a series-wound DC motor is presented in [26], with its application as an input characteristic of a motor simulation program module.

It is important to note that by applying a very similar experimental setup and procedure, the Back EMF of a Permanent Magnet Synchronous (PMS) or a Brushless DC (BLDC) motor can also be measured.

3.2. Test Measurements on an Electric Motor

In this section, two different kinds of test measurements are presented. The first one is called "locked rotor response test" or "static test", while the second one is "dynamic test". In Figure 19, an experimental setup is shown for both kinds of test measurements. The analyzed motor is a series-wound DC motor in both cases, but the setup is almost the same for any type of analyzed motor.

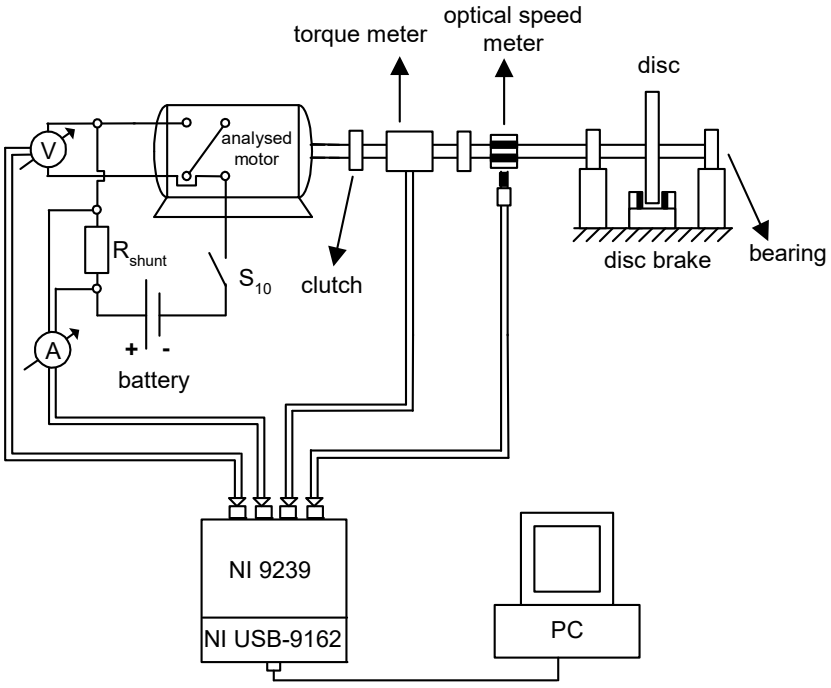

Figure 19. Experimental setup for static and dynamic test measurements.

During a "static test", the steel disc in Figure is fixed with a disc brake; thus, it cannot rotate. A "static test" is used to check the accuracy of the measured electromagnetic characteristics of the motor, as well as the proper operation of our simulation program. During the test, voltage is switched on the analyzed motor, and the time dependence of the torque, the voltage on the motor, and the intensity of the current flowing through it are measured. The results of a "static test" on a series-wound DC motor are presented in [26] and compared with simulation results.

During a "dynamic test", the steel disc in Figure can freely rotate. A "dynamic test" is used to check the accuracy of the measured dynamics characteristics of the motor, as

well as the proper operation of our simulation program. During the test, voltage is switched on the analyzed motor, and the rotor spins up from rest until it reaches its maximum speed. During the spinning up, the time dependence of its angular speed, the torque, the voltage on it, and the intensity of the current flowing through it are measured. The results of a "dynamic test" on a series-wound DC motor are presented in [27] and compared with simulation results.

In the case of a "dynamic test"—instead of the steel disc—the three-phase induction motor can also be used as a loading (C8, Section 2.2). Figure 20 shows the experimental arrangement which is used in this case.

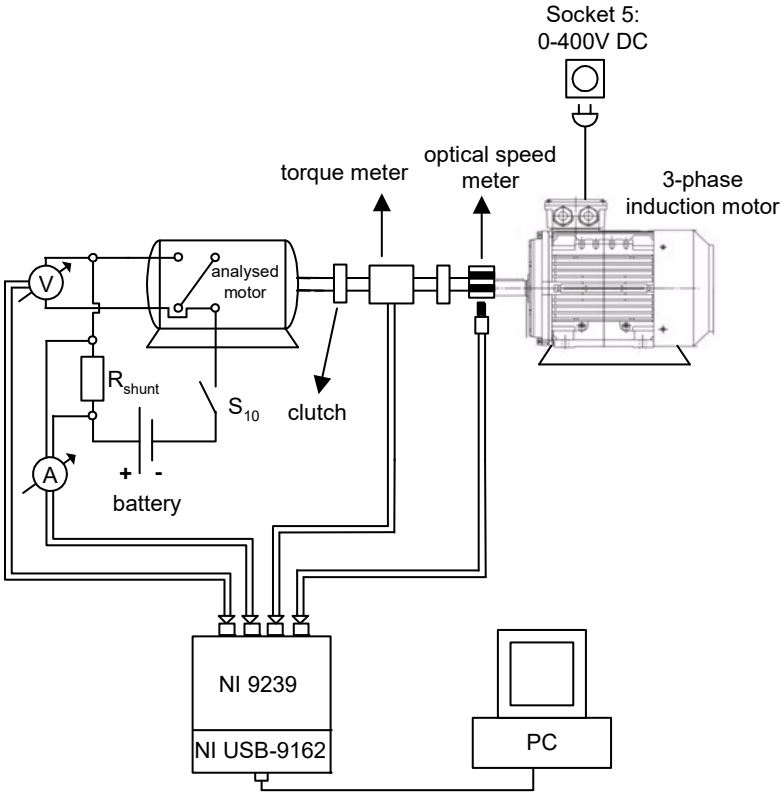

Figure 20. Application of the three-phase induction motor as loading during dynamic tests.

Varying the DC supply voltage (0–400 V) of the "load motor", the braking torque applied on the analyzed motor can be varied.

4. Conclusions

A detailed description of a recently developed complex measurement system is presented in this paper. The MS can measure the dynamics and electromagnetic characteristics of electric motors, which serve as input data for self-developed motor simulation modules. These characteristics can be, among others, the electric resistance, dynamic self and mutual inductance of motor windings, back EMF, brush voltage, braking torque and moment of inertia of the rotor. Additionally, applying the MS, test measurements can also be performed on the motors to check the accuracy of the output functions generated by the simulation modules. The maximum power that can be measured safely by the system is 4 kW. The maximum theoretical value of the measured angular speed is 250000 RPM, which is limited by the optical LED sensor. The MS, in its recent form, is capable of measuring current intensities in the range of 0–300 A and torque up to 200 Nm (the accuracy class of the torque sensor is 0.5%). As examples of the application of the MS, several experimental arrangements and procedures for specific experimental tasks were also presented here. These examples are helpful for users who deal with the study of electric motors, including

their dynamic modelling and simulation. It should be emphasized that the range of applications is continuously expanding, and some new applications may require further measurement system development. Shortly, we intend to study different types of modern electric motors, including a PMSM and a BLDC motor, applying the MS. The development of the necessary motor simulation program modules is in progress.

Author Contributions: Conceptualization, G.Á.S. and J.K.; Data curation, A.S. and É.Á.; Investigation, G.Á.S., A.S., G.J. and É.Á.; Methodology, G.Á.S., A.S., J.K. and G.J.; Software, É.Á.; Supervision, G.Á.S.; Validation, G.Á.S.; Writing – original draft, G.Á.S., A.S. and É.Á. All authors have read and agreed to the published version of the manuscript.

Funding: This research was funded by Thematic Excellence Programme, grant number [TKP2020-NKA-04]. This research was funded by NEW NATIONAL EXCELLENCE PROGRAM OF THE MINISTRY FOR INNOVATION AND TECHNOLOGY FROM THE SOURCE OF THE NATIONAL RESEARCH, DEVELOPMENT AND INNOVATION FUND, grant number [ÚNKP-21-3, ÚNKP-21-4-II].

Acknowledgements: SUPPORTED BY THE ÚNKP-21-3, ÚNKP-21-4-II NEW NATIONAL EXCELLENCE PROGRAM OF THE MINISTRY FOR INNOVATION AND TECHNO LOGY FROM THE SOURCE OF THE NATIONAL RESEARCH, DEVELOPMENT AND INNOVATION FUND. . The research was supported by the Thematic Excellence Programme (TKP2020-NKA-04) of the Ministry for Innovation and Technology in Hungary.

Conflicts of Interest: The authors declare no conflict of interest.

References

1. Li, S. A review of electric motor drives for applications in electric and hybrid vehicles. *Researchgate* **2017**.
2. De Santiago, J.; Bernhoff, H.; Ekergård, B.; Eriksson, S.; Ferhatovic, S.; Waters, R.; Leijon, M. Electrical motor drivelines in commercial all-electric vehicles: A review. *IEEE Trans. Veh. Technol.* **2011**, *61*, 475–484.
3. Dorji, C. Review Of Electric Motor Drives. *Researchgate* **2015**.
4. Xu, Y.; Zhang, H.; Yang, F.; Tong, L.; Yan, D.; Yang, Y.; Wang, Y.; Wu, Y. Experimental investigation of pneumatic motor for transport application. *Renew. Energy* **2021**, *179*, 517–527.
5. Flis, K.; Pobędza, J. Simulation of pneumatic motor used in pneumobile. *J. KONES* **2014**, *21*, 89–96.
6. Gábora, A.; Síki, G.Á.; Szántó, A.; Varga, T.A.; Magyari, A.; Balázs, D. Prototípus elektromos tanulmányautó fejlesztése a Shell Eco-Marathon® versenyre. In Proceedings of the XXII-th Scientific Conference of Young Engineers, Cluj-Napoca, Romania, 23 March 2017; Transylvanian Museum Society, Department of Technical Sciences: Cluj-Napoca, Romania, 2017; ISSN 2393–1280.
7. Szántó, A.; Síki, G.Á.; Hajdu, S.; Gábora, A.; Sipos, K.B. Járműdinamikai szimuláció és optimalizáció. *Műszaki Tudományos Közlemények* **2018**, *9*, 219–222.
8. Gábora, A.; Sipos, K.B.; Lovadi, G.D.; Szántó, A.; Síki, G.Á.; Borzan, M. Pneumatikus meghajtású tanulmányautó vesztességeinek elemzése. In Proceedings of the XXIII-rd Scientific Conference of Young Engineers, Cluj-Napoca, Romania, 17 March 2018.; Transylvanian Museum Society, Department of Technical Sciences: Cluj-Napoca, Romania, 2018; ISSN 2393–1280.
9. György, J. A Pneumobil Versenyek És Az Oktatás A Felkészülés Tanári Szemmel. *Debr. Műszaki Közlemények* **2011**, *10*, 35–40.
10. Szántó, A.; Hajdu, S.; Sziki, G.Á. Dynamic simulation of a prototype race car driven by series wound DC motor in Matlab-Simulink. *Acta Polytech. Hung.* **2020**, *17*, 103–122.
11. Szántó, A.; Síki, G.Á.; Hajdu, S.; Gábora, A. Soros gerjesztésű egyenáramú motor szimulációja MATLAB környezetben. In Proceedings of the XXII-th Scientific Conference of Young Engineers, Cluj-Napoca, Romania, 23 March 2017; Transylvanian Museum Society, Department of Technical Sciences: Cluj-Napoca, Romania, 2017; ISSN 2393–1280.
12. Síki, G.Á.; Szántó, A.; Mankovits, T. Dynamic modelling and simulation of a prototype race car in MATLAB/Simulink applying different types of electric motors. *Int. Rev. Appl. Sci. Eng.* **2021**, *12*, 57–63.
13. Szántó, A.; Szántó, A.; Sziki, G.Á. Review of the modelling methods of series wound DC motors. *Műszaki Tudományos Közlemények* **2020**, *13*, 166–169.
14. Hadžiselimović, M.; Blaznik, M.; Štumberger, B.; Zagradišnik, I. Magnetically nonlinear dynamic model of a series wound DC motor. *Przegląd Elektrotechniczny* **2011**, *87*, 60–64.
15. El Shewy, H.M.; Abd Al Kader, F.E.; El Kholy, M.M.; El Shahat, A. Dynamic modeling of permanent magnet synchronous motor using MATLAB-simulink. In Proceedings of the International Conference on Electrical Engineering ICEENG 2008, Cairo, Egypt, 27–29 May 2008; Military Technical College: Cairo, Egypt; Volume 6, pp. 1–16.
16. Zhou, Y.; Jiang, H.K.; Zhou, Q.X.; Zhang, Q.J. A Novel method for modeling and simulation of brushless DC motor with Kalman filter. In *Advanced Technology in Teaching*; Wei, Z., Ed.; Springer, Berlin/Heidelberg, Germany, 2012; pp. 305–314.

17. Shi, K.L.; Chan, T.F.; Wong, Y.K.; Ho, S.L. Modelling and simulation of the three-phase induction motor using Simulink. *Int. J. Electr. Eng. Educ.* **1999**, *36*, 163–172.
18. Aktaibi, A.; Rahman, M.A. Dynamic simulation of a three-phase induction motor using matlab simulink. In Proceedings of the 20th Annual Newfoundland Electrical and Computer Engineering Conference (NECEC 2011), St. Johns, NL, Canada, 1 November 2011. https://doi.org/10.13140/RG.2.1.2705.4243
19. Brinovar, I.; Srpčič, G.; Hadžiselimović, M.; Goričan, V.; Štumberger, B. Measurement systems for determining the characteristics of electrical machines. In Proceedings of the IEEE 2017 International Conference on Modern Electrical and Energy Systems (MEES), Kremenchuk, Ukraine, 15–17 November 2017; pp. 40–43.
20. Izhar, T.; Ali, M.; Sohaib, M.; Nazir, A. Development of a motor test bench to measure electrical/mechanical parameters. In Proceedings of the IEEE 2017 International Conference on Energy Conservation and Efficiency (ICECE), Lahore, Pakistan, 22–23 November 2017; pp. 64–67.
21. Fuengwarodsakul, N.H.; Bauer, S.E.; De Doncker, R.W. Characteristic measurement system for automotive class switched reluctance machines. *EPE J.* **2006**, *16*, 44–52.
22. Braier, Z.; Klouček, P. System of measurement and evaluation of AC servo motor's mechanic, electric and control quantities. In Proceedings of the 2015 IEEE International Workshop of Electronics, Control, Measurement, Signals and their Application to Mechatronics (ECMSM), Liberec, Czech Republic, 22–24 June 2015; pp. 1–5.
23. Schupbach, R.M.; Balda, J.C. A versatile laboratory test bench for developing powertrains of electric vehicles. In Proceedings of the IEEE 56th Vehicular Technology Conference, Vancouver, BC, Canada, 24–28 September 2002; Volume 3, pp. 1666–1670.
24. Rassõlkin, A.; Vodovozov, V. A test bench to study propulsion drives of electric vehicles. In Proceedings of the IEEE 2013 International Conference-Workshop Compatibility And Power Electronics, Ljubljana, Slovenia, 5–7 June, 2013; pp. 275–279.
25. Ádámkó, É.; Szántó, A.; Sziki, G.Á. Software developments for an electric motor test bench developed at the Faculty of Engineering of the University of Debrecen. In Proceedings of the 6th Agria Conference on Innovative Vehicle Technologies and Automation Solutions (InnoVeTAS 2022) Eger, Hungary, 13 May 2022; IOP Conference Series: Materials Science and Engineering; IOP Publishing: Bristol, UK; Volume 1237, p. 012012.
26. Sziki, G.Á.; Sarvajcz, K.; Kiss, J.; Gál, T.; Szántó, A.; Gábora, A.; Husi, G. Experimental investigation of a series wound dc motor for modeling purpose in electric vehicles and mechatronics systems. *Measurement* **2017**, *109*, 111–118.
27. Szántó, A.; Kiss, J.; Mankovits, T.; Szíki, G.Á. Dynamic Test Measurements and Simulation on a Series Wound DC Motor. *Appl. Sci.* **2021**, *11*, 4542.
28. Podzharenko, V.A.; Kucheruk, V.Y. New method of measurement of a moment of inertia of an electrical machines. In Proceedings of the XIV IMEKO World Congress, Tampere, Finland, 2–6 June 1997; Volume 3.
29. Egorov, A.V.; Kozlov, K.E.; Belogusev, B.N. Experimental identification of the electric motor moment of inertia and its efficiency using the additional inertia. *ARPN J. Eng. Appl. Sci.* **2016**, *11*, 10582–10588.
30. Rao, M.V.K. *Brush Contact Drop in D.C. Machines*; Bangalore Press: Bengaluru, India, 1934.